Published as: *Dev Cell*. 2010 November 16; 19(5): 740–752.

The Fz-Dsh planar cell polarity pathway induces oriented cell division via Mud/NuMA in *Drosophila* and zebrafish

Marion Ségalen[1,6], **Christopher A. Johnston**[4,5], **Charlotte A. Martin**[1], **Julien G. Dumortier**[2,3], **Kenneth E. Prehoda**[5], **Nicolas B. David**[2,3], **Chris Q. Doe**[4,7], and **Yohanns Bellaïche**[1,7]

[1]Polarity Division and Morphogenesis, Institut Curie, CNRS UMR 3215, INSERM U934, 26 rue d'Ulm, 75248 Paris Cedex 05, France

[2]Institut de Biologie de l'Ecole Normale Supérieure (IBENS)

[3]INSERM U1024, 75005 Paris, France

[4]Institutes of Neuroscience and Molecular Biology, HHMI, Univ. Oregon, Eugene, OR 97403 USA

[5]Institute of Molecular Biology and Department of Chemistry, Univ. Oregon, Eugene OR 97403 USA

SUMMARY

The Frizzled receptor and Dishevelled effector regulate mitotic spindle orientation in both vertebrates and invertebrates, but how Dishevelled orients the mitotic spindle is unknown. Using the *Drosophila* S2 cell "induced polarity" system, we find that Dishevelled cortical polarity is sufficient to orient the spindle, and that Dishevelled's DEP domain mediates this function. This domain binds a C-terminal domain of Mud (the *Drosophila* NuMA ortholog), and Mud is required for Dishevelled-mediated spindle orientation. In *Drosophila*, Frizzled-Dishevelled planar cell polarity (PCP) orients the sensory organ precursor (pI) spindle along the anterior-posterior axis. We show that Dishevelled and Mud colocalize at the posterior cortex of pI, Mud localization at the posterior cortex requires Dsh, and Mud loss-of-function randomizes spindle orientation. During zebrafish gastrulation, the Wnt11-Frizzled-Dishevelled PCP pathway orients spindles along the animal-vegetal axis, and reducing NuMA levels disrupts spindle orientation. Overall, we describe a Frizzled-Dishevelled-NuMA pathway that orients division from Drosophila to vertebrates.

INTRODUCTION

Oriented cell division is important for the specification of cell fate and for tissue morphogenesis (Keller, 2006; Lecuit and Le Goff, 2007; Siller and Doe, 2009). The orientation of cell division relies on intrinsic or extrinsic cortical polarity cues, which specify the orientation of the mitotic spindle. In both vertebrates and invertebrates, the Frizzled (Fz) planar cell polarity (PCP) pathway acts to orient the cell division relative to extrinsic cues within a tissue. By doing so, the Fz PCP pathway has fundamental roles in

[7]Corresponding authors: cdoe@uoneuro.uoregon.edu, yohanns.bellaiche@curie.fr.
[6]Present address: « Cellules épithéliales et morphogenèse chez C. elegans », CNRS FRE3144 - Centre de Génétique Moléculaire (CGM), Gif-sur-Yvette, France

body plan specification, cell fate determination and tissue elongation (reviewed in Segalen and Bellaïche, 2009).

Here we study the mechanism of Fz PCP regulated mitotic spindle orientation in *Drosophila* and zebrafish. During the development of the *Drosophila* adult peripheral nervous system, the sensory organ precursor (pI) divides with an anterior-posterior planar polarity to produce a posterior cell, pIIa, and an anterior cell, pIIb, which will further divide to generate, respectively, the external and internal cells of the adult mechanosensory organs (Gho and Schweisguth, 1998; Gho et al., 1999; Fichelson and Gho, 2003). The transmembrane receptor Frizzled (Fz) and its cortical effector Dishevelled (Dsh) are localized to the apical posterior cortex of the pI cell. They specify the posterior localization of the Par complex (Bazooka, Baz; Par-6; atypical protein kinase C, aPKC) and the anterior localization of the Discs large (Dlg)/Partner of Inscuteable (Pins) complex, which are both necessary to promote anterior localization of the cell fate determinants Numb and Neuralized, as well as the adaptor Partner of Numb (Pon) (Bellaïche et al., 2001a; Bellaïche et al., 2001b; Le Borgne and Schweisguth, 2003; Wirtz-Peitz et al., 2008). Spindle orientation along the anterior-posterior polarity axis does not require the Par complex, Pins, or Dlg; in contrast, Fz and Dsh are both required for spindle orientation along this polarity axis and thereby promote the correct specification of the pI daughter cells (Bellaïche et al., 2001a; Bellaïche et al., 2001b; David et al., 2005). In vertebrates, the function of PCP signaling as a regulator of mitotic spindle has been established for symmetric cell division during zebrafish gastrulation. In the epiblast, which gives rise to the neural ectoderm and the epidermis, the Wnt PCP pathway controls convergence extension cell movements and orients the mitotic spindle of dividing epiblast cells along the animal-vegetal axis, promoting the anterior-posterior elongation of the gastrulating zebrafish embryo (Concha and Adams, 1998; Heisenberg et al., 2000; Gong et al., 2004; Roszko et al., 2009). The established role of PCP in oriented cell division implies that a better understanding of how PCP links to the mitotic spindle is an important step for understanding cell fate specification and embryo morphogenesis in invertebrates and vertebrates.

Although little is known about how the PCP pathway regulates spindle orientation, there has been recent progress in understanding spindle orientation mechanisms in other contexts (reviewed in Siller and Doe, 2009). In particular, the mechanisms linking intrinsic Par complex polarity cues to the mitotic spindle depend on the conserved GoLoco domain proteins Pins/LGN/AGS3/GPR-1/2 (*Drosophila* Pins, Partner of Inscuteable; vertebrates LGN and AGS3; *C. elegans* GPR-1/2; for review Gönczy, 2008; Siller and Doe, 2009). Once localized at the cell cortex, Pins/LGN/AGS3/GPR1/2 directly bind the coiled-coil domain protein Mud/NuMA/Lin-5 (Mud, Mushroom body defective; NuMA, Nuclear Mitotic Apparatus) that recruits the dynein complex to regulate mitotic spindle orientation during *Drosophila* and *C. elegans* asymmetric cell division and spindle oscillation in human cultured cells (Grill et al., 2001; Srinivasan et al., 2003; Grill et al., 2003; Du and Macara, 2004; Schmidt et al., 2005; Bowman et al., 2006; Izumi et al., 2006; Siller et al., 2006; Nguyen-Ngoc et al., 2007; Park and Rose, 2008; Siller and Doe, 2008; Cabernard and Doe, 2009). In addition, *Drosophila* Pins can interact with the mitotic spindle via the Dlg-Khc73 pathway (Siegrist and Doe, 2005; Johnston et al., 2009). Here we show that *Drosophila* Dsh interacts with Mud protein, linking the conserved Fz-Dsh planar cell polarity pathway to the Mud/NuMA-Dynein spindle orientation pathway. Furthermore, we show that the combined Fz-Dsh-NuMA/Mud pathway regulates spindle orientation during both *Drosophila* asymmetric cell division and zebrafish tissue morphogenesis. Hence our work identifies a conserved mechanism controlling mitotic spindle orientation by extrinsic polarity cues.

RESULTS and DISCUSSION

The Dsh DEP domain is sufficient for spindle orientation in *Drosophila* S2 cells

To directly examine the role of Dsh in mitotic spindle orientation, we utilized a recently developed "induced cell polarity" system (Johnston et al., 2009). This system allows the generation of Dsh cortical asymmetric localization in the otherwise unpolarized *Drosophila* S2 cell line. It therefore allows us to test whether Dsh asymmetric distribution is sufficient to orient the spindle and if so, to identify putative Dsh effectors needed to regulate mitotic spindle orientation. Briefly, Dsh was fused in frame to the cytoplasmic terminus of the homophilic cell adhesion molecule Echinoid (Ed::Dsh), expressed in the normally non-adherent S2 cell line, and gently shaken to induce Ed-dependent cell clustering. This results in the localization of Dsh to a defined cortical domain at the site of cell-cell contact. The ability of the Dsh cortical domain to orient the mitotic spindle was assayed by measuring the mitotic spindle angle relative to the center of the Dsh cortical domain (Figure 1A; Johnston et al., 2009), and represented as a cumulative plot of spindle angle from 0° (perfectly oriented) to 90° (not oriented). In this system, random spindle orientation would give an average spindle angle of ~45° and show a linear diagonal cumulative plot spanning 0–90°, whereas a cortical domain with spindle orientation ability should give a lower average spindle angle, and a leftward deflection of the cumulative plot due to overrepresentation of small spindle angle datapoints.

We confirmed our previous findings that control S2 cells expressing Ed::GFP have randomized spindles (Figure 1B; average angle = 53° ± 23°; linear cumulative plot, Figure 1M; Table 1; Johnston et al., 2009). In contrast, fusion of the full length Dsh protein to Ed resulted in an Ed::Dsh cortical domain that had significant spindle orientation activity (Figure 1C ; average angle = 28° ± 18°; left-shifted cumulative plot, Figure 1M; Table 1). We next used this system to identify the Dsh domain responsible for spindle orientation. Dsh harbors at least three conserved domains, a DIX domain, a PDZ domain and a DEP domain (Figure 2A). The DIX and PDZ domains are sufficient to mediate canonical Wnt signaling, and the DEP domain is essential for Dsh PCP signaling activity (Axelrod et al., 1998). We found that the PDZ domain had no spindle orientation activity (Figure 1D; average spindle angle = 49° ± 24°; Figure 1M; Table 1); in contrast, the C-terminal region containing the DEP domain provided excellent spindle orientation (Figure 1E; average angle = 17° ± 15°; Figure 1M; Table 1). Expression of the N-terminal DIX domain did not result in reliable cortical targeting, thus preventing direct assessment of this domain in isolation. The finding that the isolated DEP domain is better at spindle orientation than the full length Dsh protein suggests that there may be intramolecular or intermolecular interactions in the Dsh protein that partially limit the ability of the DEP domain to orient the spindle. We next examined the ability of Fz, the canonical receptor-mediated activator of Dsh, to induce spindle orientation. Interestingly, the Fz1 C-terminal cytoplasmic domain fused to Ed did not orient the spindle in the S2 assay (Figure 1F; average angle = 46° ± 29°; Figure 1N; Table 1), despite the presence of endogenous Dsh protein in S2 cells (data not shown). However, we found that a similar fragment of Fz4 elicited spindle orientation indistinguishable from full-length Dsh (Figure 1G; average angle = 24° ± 12°; Figure 1N; Table 1). Fz4 was also capable of recruiting Dsh to the cortical Ed crescent (Figure 1K–L”). Fz1 may require cell type-specific posttranslational modifications for Dsh-mediated spindle orientation not available in S2 cells. We conclude that the Dsh DEP domain acts downstream of Fz signaling and is sufficient for spindle orientation in *Drosophila* S2 cells.

Dsh acts via the Mud-Dynein pathway to promote spindle orientation

We next sought to delineate the downstream signaling pathway(s) responsible for Dsh-mediated spindle orientation. We had previously shown that two pathways are needed for

spindle orientation in *Drosophila* S2 cells and neuroblasts: a Pins-Dlg-Khc-73 pathway, and a Pins-Mud-Dynein pathway (Johnston et al., 2009). We examined the requirement for each of these pathways in Dsh-mediated spindle-orientation using Dlg and Mud inactivation by RNAi. Whereas treatment with RNAi against Dlg did not reduce Dsh spindle orientation activity, knockdown of Mud completely abolished Dsh-mediated spindle alignment (average angle, 46° ± 27°; Figure 1H, 1I and 1O; Table 1). RNAi against Lis-1, a functional component of the dynein complex during asymmetric cell division (Nguyen-Ngoc et al., 2007; Siller and Doe, 2008), also abrogated proper spindle alignment to the Ed::Dsh crescent (Figure 1J; average angle = 43° ± 25°; Figure 1O; Table 1). We conclude that Dsh requires the Mud-Dynein pathway for its spindle orientation function in S2 cells.

Dsh and the Mud C-terminus can associate in a protein complex

To explore the mechanisms by which Dsh orients the mitotic spindle via Mud, we tested whether these proteins could associate with each other. We determined that a C-terminal region of Mud from amino acid 1825 to 2475 specifically immunoprecipates Dsh::Myc (Figure 2B and 2C) from lysate of HEK293 cells, usually used to analyze *Drosophila* PCP protein interactions (Jenny et al., 2005). This region (thereafter referred to as MudC) includes the Pins binding domain and the MT-binding domain of Mud (Bowman et al., 2006; Izumi et al., 2006; Siller et al., 2006). Furthermore, and in agreement with the results of the spindle orientation assay, the C-terminal Dsh domain containing the Dsh DEP domain is immunoprecipitated with MudC whereas the Dsh DIX-PDZ domains only weakly interact with MudC (Figure 2D). We conclude that the Dsh DEP dictates association with Mud, consistent with a role of the Dsh DEP domain in engaging the Mud-Dynein pathway for spindle orientation.

Dsh recruits Mud to the posterior cortex during pI asymmetric cell division

In order to explore the *in vivo* function of the Fz-Dsh-Mud spindle orientation pathway, we first analyzed the respective localization of Mud and Dsh during the asymmetric cell division of the *Drosophila* sensory organ precursor cell (pI, identified by the expression of Senseless (Ss), Nolo et al., 2000).

In the epithelial cells of the pupal dorsal thoracic imaginal disc, Fz and Dsh are planar polarized and they accumulate at the apical posterior cell cortex at the level of the adherens junctions (AJs) stained by Armadillo (Arm, *Drosophila* β-catenin). Fz and Dsh also strongly accumulate at the apical posterior cortex of pI cells in late interphase and prophase (Figure 3A–A”, 3C’ and 3E’ and not shown; Bellaïche et al., 2004; David et al., 2005). There, they colocalized with Mud protein (80% of the cells; n=24; Figure 3C, 3C”, 3E and 3E”). We next tested whether Dsh or Mud regulate the localization of each other in interphase/prophase pI cells. We found that the apical posterior localization of Dsh was not affected in *mud* mutant pI cells (Figure 3B–B”), whereas the apical localization of Mud was lost in dsh^{1} mutant pI cells (n=16, Figure 3D–D” and 3F–F”). The dsh^{1} allele abrogates only the Dsh PCP function (Axelrod et al., 1998) and contains a missense mutation in the DEP domain, consistent with our biochemical data showing MudC-Dsh DEP domain interaction (see above). We conclude that Dsh recruits Mud to the apical posterior cortex in interphase/prophase pI cells. In prophase, Mud could also be found to accumulate with Pins at the anterior lateral or basal cortex when Pins was enriched at the anterior cortex in early prophase in wild-type and dsh^{1} mutant pI cells (not shown and Figure 3F–F”).

In prometaphase and metaphase pI cells, Dsh accumulates at the apical posterior cortex whereas Pins accumulates at the anterior lateral cortex (Figure 3G–G”). In addition, the mitotic spindle is aligned along the anterior posterior axis (Gho et al., 1999; David et al., 2005). At the posterior cortex, Mud was partially colocalized with Dsh at the apical

posterior pI cell cortex at the level of the AJs since it is also present laterally along the pI cell cortex (n=13; Figure 3I–3I" and 3K–K'). At the anterior cortex, Mud is located laterally with Pins (n=14; Figure 3I–3I" and 3K–K"). Furthermore the posterior and anterior cortical Mud enrichments were found in close vicinity of the posterior and anterior centrosomes of the dividing pI cell, respectively (arrowheads in Figure 3I–I", 3K–K"). In *pins* mutant pI cells, the Mud anterior localization was reduced or lost (n=30; Figure 3L–L") in agreement with the previously described interaction between Mud and Pins in neuroblasts (Bowman et al., 2006; Izumi et al., 2006; Siller et al., 2006). In contrast, Mud apical posterior accumulation was maintained in *pins* null mutant pI cells in prophase (n=8, Figure 3H–H"). In dsh^1 mutant prometaphase pI cells, Mud apical and lateral posterior enrichment opposite to the Pins accumulation was reduced or lost (n=16; Figure 3J–J"), similar to the phenotype at interphase/prophase. Altogether, we conclude that in the dividing pI cells, Mud is recruited to the anterior lateral cortex by Pins, and, consistent with the observed interaction between the Dsh DEP domain and the Mud C-terminal domain, Mud is recruited to the posterior cortex by Dsh.

Mud is required for anterior-posterior spindle orientation in pI cells

The orientation of the mitotic spindle in the pI cell is strictly controlled along both the anterior-posterior axis and the apical-basal axis (Figure 4A). Fz and Dsh orient the mitotic spindle along the anterior-posterior axis but their apical localization tends to tilt the spindle relative to the apical-basal axis (Gho and Schweisguth, 1998; Bellaïche et al., 2001a; David et al., 2005). In contrast, Pins and heterotrimeric G protein (HGP) pathway, which act at the anterior lateral cortex, are only needed to counterbalance the apical-basal tilt induced by the Fz PCP pathway; thereby they maintain the mitotic spindle in the plane of the epithelium (David et al., 2005). Thus, in cells lacking the Fz PCP pathway, the spindle is both misaligned relative to the anterior-posterior axis and parallel to the plane of the epithelium, whereas in *pins* mutant pI cells, the spindle is correctly aligned along the anterior-posterior axis but is strongly tilted relative to the apical-basal axis (Figure 4A).

In order to characterize the role of Mud in the pI cell spindle orientation, we first tested whether *mud* mutants have normal pI cell polarity. Wild-type mitotic pI cells have Numb, Pon and Pins localized to the anterior cortex and Baz localized to the posterior cortex (Figure 4B–B', 4D–D', 4F–F' and 4H–H'). In *mud* mutant mitotic pI cells, all four proteins showed normal polarized localization (Figure 4C–C', 4E–E', 4G–G', 4I–I' and Supplementary Figure S1A–C). Thus, *mud* mutant pI cells have normal anterior-posterior cortical polarity, permitting us to analyze the function of Mud in spindle orientation.

We assayed pI mitotic spindle orientation in living *Drosophila* pupa by expressing the microtubule-associated Tau::GFP fusion protein in pI cells using the *neuralized-GAL4* driver (Bellaïche et al., 2001a; David et al., 2005). We measured the angle of the spindle relative to both the anterior-posterior axis (α_{AP}) and the angle of the spindle relative to the plan of the epithelium (α_{AB}) (Figure 4A; David et al., 2005) in wild type, dsh^1, *mud* or *pins* mutant pI cells. In *mud* mutant pI cells, the mitotic spindle was parallel to the plane of the epithelium (mean $\alpha_{AB mud}$=3.2° ± 19°, $p_{wt/mud}$=0.003, Figure 4J); a similar phenotype was observed for *dsh* and *fz* mutant pI cells ($p_{dsh/mud}$=0.56; $p_{fz/mud}$=0.34, Figure 4J and not shown). This phenotype is distinct from the one observed in *pins* or HGP pathway mutant pI cells ($p_{pins/mud}$ =0.0001 and $p_{G\alpha i/mud}$ =0.0001, Figure 4J and not shown). Furthermore, the orientation of the mitotic spindle was randomized relative to the anterior-posterior axis in *mud* mutant pI cells ($p_{WT/mud}$=0.0009, Figure 4K) similar to *dsh* or *fz* mutant pI cells ($p_{mud/dsh}$=0.31, $p_{mud/fz}$=0.47, Figure 4K and not shown). This suggests that Mud does not simply function downstream of Pins, as previously reported (Bowman et al., 2006; Izumi et al., 2006; Siller et al., 2006), but rather that it might act in the same pathway as Fz and Dsh. The observation that Dsh recruits Mud to the apical posterior cortex, and that *fz*, *dsh*, and

mud mutants share a common spindle orientation phenotype, leads us to propose that Mud acts downstream of the Fz-Dsh PCP pathway to regulate anterior-posterior mitotic spindle orientation in pI cells.

To analyze the cell fate consequences of *mud* mutant spindle orientation defects in pI cells, we analyzed the segregation of Partner of Numb::GFP (Pon::GFP) in pI cells expressing Histone2B::mRFP by time-lapse microscopy. In wild-type cells, Pon::GFP accumulates at the anterior cortex of the pI cell in metaphase and segregates only into the anterior daughter cell in telophase (n=17, Figure 5A). In 27% of *mud* mutant pI cells in telophase (n=15), Pon::GFP failed to exclusively segregate in one of the two daughter cells (Figure 5B). Accordingly, the loss of Mud function was associated with pIIb to pIIa cell fate misspecification as marked by the presence of sensory organs only composed of external sensory cells at the expense of the internal sensory cells (Figure 5C–5F"). Thus, Mud is required for the proper specification of pI daughter cells as an effector of Fz signaling during asymmetric cell division.

Mud has been shown to function downstream of Pins in *Drosophila* neuroblasts. To analyze whether Mud could also function downstream of Pins in absence of PCP activity, we compared the orientation of the mitotic spindle relative to the Pins crescent in dsh^1 versus dsh^1, *mud* mutant pI cells (Supplementary Figure S1D–I). Whereas the mitotic spindle was aligned with the Pins crescent in most of the dsh^1 mutant pI cells in metaphase, the mitotic spindle failed to align with the Pins crescent in dsh^1, *mud* double mutant pI cells in metaphase. We conclude that Mud functions downstream of Fz signaling to regulate mitotic spindle orientation and that, in absence of Fz activity, Mud is needed downstream of Pins to orient the mitotic spindle in the pI cell.

NuMA is required for Dsh-dependent mitotic spindle orientation during zebrafish gastrulation

The vertebrate NuMA protein, ortholog of *Drosophila* Mud protein, has never been tested for a role in spindle orientation during tissue development. NuMA is a good candidate for regulating spindle orientation in vertebrate embryos because it is known to regulate mitotic spindle oscillation in cultured cells (Du and Macara, 2004), it is asymmetrically localized during skin and neuron progenitor asymmetric cell division (Lechler and Fuchs, 2005; Lake and Sokol, 2009), and its invertebrate orthologs are known to regulate spindle orientation (Srinivasan et al., 2003; Du and Macara, 2004; Bowman et al., 2006; Izumi et al., 2006; Siller et al., 2006; Park and Rose, 2008; Cabernard and Doe, 2009). Having established the role of Mud in the Fz-Dsh PCP spindle orientation pathway in *Drosophila*, here we analyze the function of NuMA in the zebrafish epiblast where the Wnt11 PCP pathway orients the mitotic spindle along the animal-vegetal axis during gastrulation (Gong et al., 2004).

In order to determine whether zebrafish Dishevelled (Dvl) could orient the mitotic spindle using a pathway analogous to *Drosophila* Dsh, we first tested if the zebrafish Dvl3 DEP domain has spindle orientation activity in the S2 induced polarity assay. Strikingly, Ed::Dvl3(DEP) domain orients the mitotic spindle and this spindle orientation activity requires Mud function (Figure 6A–C). This indicates that zebrafish Dishevelled acts via its DEP domain to activate the Mud-Dynein spindle orientation pathway in S2 cells. We next sought to determine whether Dvl3 could associate with zebrafish NuMA and whether they might colocalize in zebrafish epiblast cells. We identified the zebrafish NuMA gene, which is encoded by a 7.1 kb mRNA. Zebrafish NuMA, like Dvl3, is ubiquitously expressed in the epiblast during gastrulation (Thisse and Thisse, 2004 and Supplementary Figure S2A–F). We determined that a C-terminal fragment of zebrafish NuMA from amino acid 1508 to 2382 (NuMAC) specifically immunoprecipitates Dvl3::Myc (Figure 6D) from lysate of HEK293 cells. In interphase and dividing epiblast cells Dvl3::GFP was mostly localized in

the cytoplasm. In interphase, HA::NuMAC was localized in the nucleus and did not colocalize with Dvl3::GFP (Figure 6E–E"). During cell division, HA::NuMAC was mostly cytoplasmic (Figure 6E–E"). We could nevertheless observe localization of HA::NuMAC at the cell cortex in about half of the cells (Figure 6E'–E"). In division Dvl3::GFP was mostly cytoplasmic (Wallingford et al., 2000 and Figure 6E), preventing assessment of its colocalization with HA::NuMAC (Figure 6E"). Strikingly, co-injection of Fz7 induced the recruitment of Dvl3::GFP to the cell cortex as well as a translocation of HA::NuMAC from the cytoplasm to the cell cortex, where it was colocalized with Dvl3::GFP (Figure 6F–F"). In this context, Dvl3::GFP and HA::NuMAC were also found to colocalize in cytoplasmic structures such as the mitotic spindle. (Figure 6F") We also analyzed the colocalization between HA::NuMAC and Dvl2::GFP, finding that HA::NuMAC colocalized with Dvl2::GFP at the cell cortex and on the mitotic spindle, even without Fz7 injection (Figure 6G–G").

To test whether NuMA might function downstream of the PCP pathway *in vivo*, we then compared the effects of Dvl Morpholino (MO) and NuMA MO injection on the orientation of the mitotic spindle along the animal-vegetal axis during zebrafish gastrulation. In order to measure the orientation of cell divisions in the epiblast, the cell membranes were labeled with a GFP fused to a Ras-prenylation domain (hereafter membrane::GFP) and cell division orientation was determined by measuring the angle between the long axis of late anaphase cells and the animal-vegetal axis (Figure 6H). We confirm previous observations (Gong et al., 2004) that cell divisions are preferentially oriented along the animal-vegetal axis in wild-type embryos (Figure 6K). In contrast, injection of a mRNA coding for a dominant-negative form of Xenopus Dishevelled (Xdd1) led to the misorientation of the mitotic spindle relative to animal-vegetal axis in embryos ($p_{wt/Xdd1}$=0.003, Figure 6K). The function of Dvl in the regulation of mitotic spindle orientation along the animal-vegetal axis was further analyzed by the co-injection of MO against the three identified zebrafish Dishevelled, Dvl2, Dvl3 and Dvl2-like. Triple Dvl MO randomized the orientation along the animal-vegetal axis ($p_{ctrl\ MO/3Dvl\ MO}$ =0.001, Figure 6I, 6K and 6M). In vertebrates, NuMA has essential functions in nuclear organization, mitotic spindle formation and mitotic exit (Radulescu and Cleveland, 2010). We therefore induced a partial loss of function of NuMA by injection of 0.6 pmol of NuMA MO allowing the study of the role of NuMA during gastrulation. At this concentration, NuMA MO does not lead to any defect in mitotic spindle morphology (Supplementary Figure S2I–J") or to any gross morphological defects during embryonic development. In particular embryo elongation was normal suggesting that NuMA loss of function does not induce obvious convergence-extension defects (not shown). Upon injection of 0.6 pmol of NuMA MO, the mitotic spindle was significantly less oriented along the animal-vegetal axis, whereas the mitotic spindle orientation was normal in embryos injected with a control 5-mismatch MO (9 embryos for a total of 339 divisions analyzed, $p_{ctrl\ MO/NuMA\ MO}$ =0,0001, Figure 6J and 6L). The specificity of the defects in spindle orientation induced by NuMA MO was further established by showing that a second independent MO, targeting a distinct sequence of NuMA, produces the same phenotype (Figure 6L). Thus, triple Dvl MO and the NuMA MO both disrupt mitotic spindle orientation along the animal-vegetal axis, although the NuMA MO phenotype is slightly less severe. This less severe phenotype is likely due to the partial loss of NuMA function induced by MO, however we can not rule out that other regulators of mitotic spindle orientation function downstream of Fz PCP in zebrafish (Figure 6M). Altogether, we conclude that NuMA is required downstream of the Fz PCP pathway to orient symmetric cell division in zebrafish.

Conclusion

Oriented cell division has a fundamental role in cell fate specification, tissue morphogenesis and homeostasis. The orientation of cell division has been extensively characterized downstream of the Pins/LGN/AGS3/Lin-5 protein family that regulates spindle orientation in response to cell intrinsic cues during asymmetric cell division in *Drosophila* and *C. elegans*. In contrast the mechanisms regulating mitotic spindle relative to extrinsic polarity cues associated with cell-cell contact or epithelial planar cell polarity are poorly understood. Here we have deciphered the mechanisms of mitotic spindle orientation in response to the PCP signaling. Using the recently developed "induced polarity" S2 cell system, we show that the Dsh DEP domain is sufficient for spindle orientation, and that it requires Mud and Dynein complex function. We show that the Dsh DEP domain can immunoprecipitate the Mud C-terminal domain, and that the Dsh DEP domain is required to recruit Mud to the apical posterior cortex of pI cells. We propose that *Drosophila* pI cells use a Fz-Dsh-Mud-Dynein pathway for anterior-posterior spindle orientation; this pathway operates in parallel to the previously identified Pins-Mud-Dynein pathway regulating apical-basal spindle orientation. Finally, we document the functional relevance and conservation of this pathway in vertebrates. Our work generalizes the role of NuMA as regulator of mitotic spindle orientation in response to intrinsic and extrinsic polarity cues by establishing a molecular and functional characterization of a Fz-Dsh-NuMA pathway orienting cell division both in *Drosophila* and zebrafish.

EXPERIMENTAL PROCEDURES

S2 cell experiments

S2 cells were grown and cultured at room temperature in Schneider's Insect Media (Sigma) supplemented with 10% fetal bovine serum. The "induced cell polarity" assay was carried out as previously described (Johnston et al., 2009). Briefly, ~1 × 10^6 cells were transiently transfected with Ed fusion constructs (~400 ng) using Effectene (Qiagen) reagent according to manufacturer protocol. Following 24–48 hour transfection, cells were induced with $CuSO_4$ (500 μM) for 24 hours to allow for Ed fusion protein expression. Cells were harvested and resuspended in fresh media and allowed to shake (175 RPM) for 2–3 hours to induce Ed-mediated cell-cell clusters. Clustered cells were plated on glass coverslips and allowed to incubate for 3 hours to allow for optimal mitotic index. Cells were fixed (4% PFA in PBS for 15 minutes) and stained using standard techniques (Johnston et al., 2009) prior to imaging.

Immunoprecipitation

HEK293T cells were grown in DMEM supplemented with 10% Fetal Calf Serum. Immunoprecipitation were carried out as previously described in Langevin et al., 2005b. Briefly, HEK 293T were transfected with Drosophila Dsh or Mud fusion constructs or with zebrafish Dvl3 or NuMA fusion contructs. Cells were lysed in 50mM Tris-HCl (pH 8), 150 mM NaCl, 1mM EDTA, 5mM ®-glycerophosphate, 1% Triton X-100 supplemented with Complete (Roche) protease inhibitor cocktail. Mud::GFP fusion protein were immunoprecipated with mouse Anti-GFP (Roche) and Magnetic GA-sepharose agarose beads (Ademtech). Following three washes in 50mM Tris-HCl (pH 8), 150mM NaCl, 1mM EDTA, 0.1% Triton X-100, immunoprecipitates were analyzed by Western Blot using rabbit Anti-Myc antibody (Santa Cruz).

Fly stocks

Two *mud* alleles were used: mud^4 allele, a presumptive null with a nonsense mutation creating an early stop after the fifth amino acid (Guan et al., 2000) and mud^{Fo1205} a

presumptive null allele with a PiggyBac element inserted in the 5' non translated region. Mud protein is not detected by Western Blot or immunofluorescence in *mud*^{4} or *mud*^{Fo1205} mutant tissue (Harvard stock). All results obtained were similar for the two alleles. We used *pins*^{62} and *dsh*^{1} alleles that have been previously described (Axelrod et al., 1998; Yu et al., 2000). UAS-Pon::GFP (Lu et al., 1999), UAS-Histone::mRFP (Langevin et al., 2005a), UAS-Tau::GFP (Kaltschmidt et al., 2002) and *neuralized-Gal4* (Bellaïche et al., 2001a) have been previously described.

Antibodies and imaging

Antibodies used in this study were rabbit anti Mud (1/500, directed against aa 375–549, H. Nash), rabbit anti-Mud (1/500, directed against aa 1510–1693, H. Nash), rabbit anti-Mud (1/100, Batch 351-2AP,directed against aa 67–353, F. Matsuzaki), rat anti-Pins (1/100, W. Chia), guinea pig anti-Numb (1/500, Y.N. Jan), rabbit anti-Baz (1/2000, A. Wodarz), mouse anti-Senseless (1/500, Agrobio), rat anti-Dsh (1/1000, batch CA, T. Uemura), rat anti-α-tubulin (1/500, Abcam), mouse anti-γ-tubuline (Glu88, 1/1000, Sigma), rat anti-HA (1/200) and rabbit anti-phosphohistone-3 (1/1000, Upstate). HA tagged stainings were amplified using Tyramine amplification kit (Perkin). The Cy3- and Cy5-coupled secondary antibodies were from Jackson laboratories and Alexa-488-coupled secondary antibodies were from molecular probes. Fixed and live images acquired on Zeiss LSM 510, Zeiss LSM710 or Leica SP2.

Zebrafish *in situ*, injection and imaging

Embryos were obtained from wild type adults, maintained and staged accordingly to Kimmel et al., 1995. The NuMA *in situ* probe was designed in the middle of the NuMA gene. The primers used for the amplification were: GAAAAGATTTCTCTTAAAGATGAAGAAATC and GAGTTCAGATTCCTTCTGGGAAGCAG. This sequence was cloned into the BamHI and EcoRI sites of the pBluescript KS vector. Zebrafish Dvl3 full length and Zebrafish NuMA (aa 1508 to 2382) were synthesized by GenScript with AttB1 site and were cloned by gateway cloning in HA or GFP vectors. The first NuMA morpholino is directed against the ATG sequence of the NuMA gene. Its sequence is: CCGCCTTGTTCTTATTAAACTTCAT. The control morpholino was created by 5 changes in the NuMA morpholino sequence: CCcCCTTcTTgTTATTAAAgTTgAT. The efficiency of the NuMA MO was controlled by showing that the expression of a GFP gene harboring the NuMA MO sequence was abrogated by NuMA MO but not by the control MO (Supplementary Figure S2G–H"). The second NuMA morpholino is directed against the 5' of the NuMA gene. Its sequence is: GCGGTCTCTAAAAAACACACATTTTT. Upon injection of more than 0.6 pmol, the NuMA morpholino induces a developmental arrest. Only embryos showing a normal development were analyzed. 1.2 pmol of each Dvl2, Dvl3 (Angers et al., 2006) and Dvl2-Like MO (GGTATATGATTTTAGTCTCCGCCAT) were co-injected. The morpholinos were synthesized by Gene tools, Philomath, OR. Zebrafish Fz7 mRNA, zebrafish Dvl2::GFP mRNA and zebrafish Dvl3::GFP mRNA were injected at 50ng/µl. HA::NuMAC mRNA was injected at 40 ng/µl. Imaging was performed on Leica DMR 6000 or Nikon Ti spinning disk microscopes equipped with a HQ2 Ropper Camera..

Statistics

Student tests were used to compare the division angle distributions for the analysis of Mud function in Drosophila pI cells. Kolmogorov-Smirnov tests were used to compare the division angle distribution in zebrafish embryos. Chi^{2} tests were used to compare the cortical localization of Mud.

Supplementary Material

Refer to Web version on PubMed Central for supplementary material.

Acknowledgments

We thank W. Chia, F. Matsuzaki, A. Merdes, H. Nash, R. Scott, M. Semeriva, D.L. Shi, T. Uemura, C. Vesque, A. Wodarz, the Developmental Studies Hybridoma Bank and the Bloomington Stock Center for strains and antibodies. We also thank the members of the Lhomond and of the Developmental Biology Curie Imaging (PICT-IBiSA@BDD, UMR3215/U934) facilities for their help and advice with confocal microscopy. We thank P.-L. Bardet, J.-R. Hyunh, A.-M. Lennon, A. Leibfried, J. Matthieu and A. Molla-Herman for critical comments on the manuscript. Y.B. thanks A. Molla-Herman for help with the figures. This work was supported by grants to Y.B. from the Association pour la Recherche sur le Cancer (ARC 4830), the ANR (BLAN07-3-207540), the CNRS, INSERM, ERC Starting Grant (CePoDro 209718) and the Curie Institute. M.S. was supported by a pre-doctoral fellowship from ARC and from French Research Ministry. This work is also supported by the FRM grant n°26329 and the INCA grant n°4731. C.A.J. is supported by a Damon Runyon postdoctoral fellowship; K.E.P. by the National Institutes of Health (NIH GM068032), and C.Q.D. by the Howard Hughes Medical Institute (HHMI).

REFERENCES

Angers S, Thorpe CJ, Biechele TL, Goldenberg SJ, Zheng N, MacCoss MJ, Moon RT. The KLHL12-Cullin-3 ubiquitin ligase negatively regulates the Wnt-beta-catenin pathway by targeting Dishevelled for degradation. Nat Cell Biol. 2006; 8:348–357. [PubMed: 16547521]

Axelrod JD, Miller JR, Shulman JM, Moon RT, Perrimon N. Differential recruitment of Dishevelled provides signaling specificity in the planar cell polarity and Wingless signaling pathways. Genes Dev. 1998; 12:2610–2622. [PubMed: 9716412]

Bellaïche Y, Beaudoin-Massiani O, Stuttem I, Schweisguth F. The planar cell polarity protein Strabismus promotes Pins anterior localization during asymmetric division of sensory organ precursor cells in Drosophila. Development. 2004; 131:469–478. [PubMed: 14701683]

Bellaïche Y, Gho M, Kaltschmidt JA, Brand AH, Schweisguth F. Frizzled regulates localization of cell-fate determinants and mitotic spindle rotation during asymmetric cell division. Nat Cell Biol. 2001a; 3:50–57.

Bellaïche Y, Radovic A, Woods DF, Hough CD, Parmentier ML, O'Kane CJ, Bryant PJ, Schweisguth F. The Partner of Inscuteable/Discs-large complex is required to establish planar polarity during asymmetric cell division in Drosophila. Cell. 2001b; 106:355–366.

Bowman SK, Neumüller RA, Novatchkova M, Du Q, Knoblich JA. The Drosophila NuMA Homolog Mud regulates spindle orientation in asymmetric cell division. Dev Cell. 2006; 10:731–742. [PubMed: 16740476]

Cabernard C, Doe CQ. Apical/basal spindle orientation is required for neuroblast homeostasis and neuronal differentiation in Drosophila. Dev Cell. 2009; 17:134–141. [PubMed: 19619498]

Concha ML, Adams RJ. Oriented cell divisions and cellular morphogenesis in the zebrafish gastrula and neurula: a time-lapse analysis. Development. 1998; 125:983–994. [PubMed: 9463345]

David NB, Martin CA, Segalen M, Rosenfeld F, Schweisguth F, Bellaïche Y. Drosophila Ric-8 regulates Galphai cortical localization to promote Galphai-dependent planar orientation of the mitotic spindle during asymmetric cell division. Nat Cell Biol. 2005; 7:1083–1090. [PubMed: 16228010]

Du Q, Macara IG. Mammalian Pins is a conformational switch that links NuMA to heterotrimeric G proteins. Cell. 2004; 119:503–516. [PubMed: 15537540]

Fichelson P, Gho M. The glial cell undergoes apoptosis in the microchaete lineage of Drosophila. Development. 2003; 130:123–133. [PubMed: 12441297]

Gho M, Schweisguth F. Frizzled signalling controls orientation of asymmetric sense organ precursor cell divisions in Drosophila. Nature. 1998; 393:178–181. [PubMed: 9603522]

Gho M, Bellaïche Y, Schweisguth F. Revisiting the Drosophila microchaete lineage: a novel intrinsically asymmetric cell division generates a glial cell. Development. 1999; 126:3573–3584. [PubMed: 10409503]

Gong Y, Mo C, Fraser SE. Planar cell polarity signalling controls cell division orientation during zebrafish gastrulation. Nature. 2004; 430:689–693. [PubMed: 15254551]

Gönczy P. Mechanisms of asymmetric cell division: flies and worms pave the way. Nat Rev Mol Cell Biol. 2008; 9:355–366. [PubMed: 18431399]

Grill SW, Gönczy P, Stelzer EH, Hyman AA. Polarity controls forces governing asymmetric spindle positioning in the Caenorhabditis elegans embryo. Nature. 2001; 409:630–633. [PubMed: 11214323]

Grill SW, Howard J, Schäffer E, Stelzer EH, Hyman AA. The distribution of active force generators controls mitotic spindle position. Science. 2003; 301:518–521. [PubMed: 12881570]

Guan Z, Prado A, Melzig J, Heisenberg M, Nash HA, Raabe T. Mushroom body defect, a gene involved in the control of neuroblast proliferation in Drosophila, encodes a coiled-coil protein. Proc Natl Acad Sci U S A. 2000; 97:8122–8127. [PubMed: 10884435]

Heisenberg CP, Tada M, Rauch GJ, Saúde L, Concha ML, Geisler R, Stemple DL, Smith JC, Wilson SW. Silberblick/Wnt11 mediates convergent extension movements during zebrafish gastrulation. Nature. 2000; 405:76–81. [PubMed: 10811221]

Izumi Y, Ohta N, Hisata K, Raabe T, Matsuzaki F. Drosophila Pins-binding protein Mud regulates spindle-polarity coupling and centrosome organization. Nat Cell Biol. 2006; 8:586–593. [PubMed: 16648846]

Jenny A, Reynolds-Kenneally J, Das G, Burnett M, Mlodzik M. Diego and Prickle regulate Frizzled planar cell polarity signalling by competing for Dishevelled binding. Nat Cell Biol. 2005; 7:691–697. [PubMed: 15937478]

Johnston CA, Hirono K, Prehoda KE, Doe CQ. Identification of an Aurora-A/PinsLINKER/Dlg spindle orientation pathway using induced cell polarity in S2 cells. Cell. 2009; 138:1150–1163. [PubMed: 19766567]

Kaltschmidt JA, Lawrence N, Morel V, Balayo T, Fernández BG, Pelissier A, Jacinto A, Martinez Arias A. Planar polarity and actin dynamics in the epidermis of Drosophila. Nat Cell Biol. 2002; 4:937–944. [PubMed: 12447392]

Keller R. Mechanisms of elongation in embryogenesis. Development. 2006; 133:2291–2302. [PubMed: 16720874]

Kimmel CB, Ballard WW, Kimmel SR, Ullmann B, Schilling TF. Stages of embryonic development of the zebrafish. Dev Dyn. 1995; 203:253–310. [PubMed: 8589427]

Lake BB, Sokol SY. Strabismus regulates asymmetric cell divisions and cell fate determination in the mouse brain. J Cell Biol. 2009; 185:59–66. [PubMed: 19332887]

Langevin J, Le Borgne R, Rosenfeld F, Gho M, Schweisguth F, Bellaiche Y. Lethal giant larvae controls the localization of notch-signaling regulators numb, neuralized, and Sanpodo in Drosophila sensory-organ precursor cells. Curr Biol. 2005a; 15:955–962. [PubMed: 15916953]

Langevin J, Morgan MJ, Rosse C, Racie V, Sibarita J, Aresta S, Murthy M, Schwarz T, Camonis J, Bellaiche Y. Drosophila Exocyst Components Sec5, Sec6, and Sec15 Regulate DE-Cadherin Trafficking from Recycling Endosomes to the Plasma Membrane. Dev Cell. 2005b; 9:365–376. [PubMed: 16224820]

Le Borgne R, Schweisguth F. Unequal segregation of Neuralized biases Notch activation during asymmetric cell division. Dev Cell. 2003; 5:139–148. [PubMed: 12852858]

Lechler T, Fuchs E. Asymmetric cell divisions promote stratification and differentiation of mammalian skin. Nature. 2005; 437:275–280. [PubMed: 16094321]

Lecuit T, Le Goff L. Orchestrating size and shape during morphogenesis. Nature. 2007; 450:189–192. [PubMed: 17994084]

Lu B, Ackerman L, Jan LY, Jan YN. Modes of protein movement that lead to the asymmetric localization of partner of Numb during Drosophila neuroblast division. Mol Cell. 1999; 4:883–891. [PubMed: 10635314]

Nguyen-Ngoc T, Afshar K, Gönczy P. Coupling of cortical dynein and G alpha proteins mediates spindle positioning in Caenorhabditis elegans. Nat Cell Biol. 2007; 9:1294–1302. [PubMed: 17922003]

Nolo R, Abbott LA, Bellen HJ. Senseless, a Zn finger transcription factor, is necessary and sufficient for sensory organ development in Drosophila. Cell. 2000; 102:349–362. [PubMed: 10975525]

Park DH, Rose LS. Dynamic localization of LIN-5 and GPR-1/2 to cortical force generation domains during spindle positioning. Dev Biol. 2008; 315:42–54. [PubMed: 18234174]

Radulescu AE, Cleveland DW. NuMA after 30 years: the matrix revisited. Trends Cell Biol. 2010; 20:214–222. [PubMed: 20137953]

Roszko I, Sawada A, Solnica-Krezel L. Regulation of convergence and extension movements during vertebrate gastrulation by the Wnt/PCP pathway. Semin Cell Dev Biol. 2009; 20:986–997. [PubMed: 19761865]

Schmidt DJ, Rose DJ, Saxton WM, Strome S. Functional analysis of cytoplasmic dynein heavy chain in Caenorhabditis elegans with fast-acting temperature-sensitive mutations. Mol Biol Cell. 2005; 16:1200–1212. [PubMed: 15616192]

Segalen M, Bellaïche Y. Cell division orientation and planar cell polarity pathways. Semin Cell Dev Biol. 2009

Siegrist SE, Doe CQ. Microtubule-induced Pins/Galphai cortical polarity in Drosophila neuroblasts. Cell. 2005; 123:1323–1335. [PubMed: 16377571]

Siller KH, Doe CQ. Lis1/dynactin regulates metaphase spindle orientation in Drosophila neuroblasts. Dev Biol. 2008; 319:1–9. [PubMed: 18485341]

Siller KH, Doe CQ. Spindle orientation during asymmetric cell division. Nat Cell Biol. 2009; 11:365–374. [PubMed: 19337318]

Siller KH, Cabernard C, Doe CQ. The NuMA-related Mud protein binds Pins and regulates spindle orientation in Drosophila neuroblasts. Nat Cell Biol. 2006; 8:594–600. [PubMed: 16648843]

Srinivasan DG, Fisk RM, Xu H, van den Heuvel S. A complex of LIN-5 and GPR proteins regulates G protein signaling and spindle function in C elegans. Genes Dev. 2003; 17:1225–1239. [PubMed: 12730122]

Thisse, Thisse. Fast Release Clones: A High Throughput Expression Analysis. ZFIN Direct Data Submission. 2004

Wallingford JB, Rowning BA, Vogeli KM, Rothbächer U, Fraser SE, Harland RM. Dishevelled controls cell polarity during Xenopus gastrulation. Nature. 2000; 405:81–85. [PubMed: 10811222]

Wirtz-Peitz F, Nishimura T, Knoblich JA. Linking cell cycle to asymmetric division: Aurora-A phosphorylates the Par complex to regulate Numb localization. Cell. 2008; 135:161–173. [PubMed: 18854163]

Yu F, Morin X, Cai Y, Yang X, Chia W. Analysis of partner of inscuteable, a novel player of Drosophila asymmetric divisions, reveals two distinct steps in inscuteable apical localization. Cell. 2000; 100:399–409. [PubMed: 10693757]

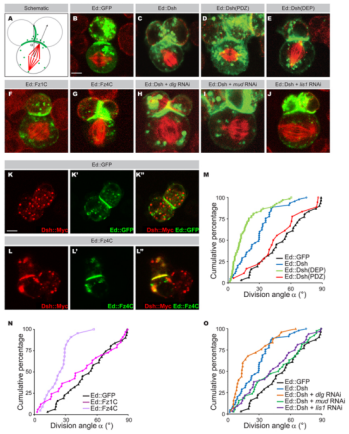

Figure 1. Dissection of the Dsh-Mud-Dynein pathway in S2 cells

A: Schematic representation of the division angle measured in S2 cells. The angle of division (α) is defined by the vector perpendicular to the middle of Ed::GFP crescent and the spindle axis.

B–J: Dsh domains were fused in frame to Echinoid tagged with GFP (green) (**C–E** and **H–J**) and transfected into S2 cells. C-terminal domain of Fz1 from amino acid 553 to 581 (**F**) and C-terminal domain of Fz4 from amino acid 560 to 705 (**G**) were fused in frame to Echinoid (Ed) (green) and transfected into S2 cells. Cells were stained for α-tubulin (red). Ed::GFP control (**B**) ; Ed::Dsh corresponds to Ed::GFP fused to Dsh full length (FL) (**C**); Ed::Dsh(PDZ) corresponds to Ed::GFP fused to the Dsh(PDZ) (**D**) ; Ed::Dsh(DEP) corresponds to Ed ::GFP fused to the Dsh(DEP) (**E**); Ed::Fz1 corresponds to Ed::GFP fused to Fz1 C-terminal domain (**F**); Ed::Fz4 corresponds to Ed::GFP fused to Fz4 C-terminal domain (**G**); Ed::Dsh + *dlg* RNAi corresponds to Ed::GFP fused to Dsh FL and RNAi against Dlg (**H**); Ed::Dsh + *mud* RNAi corresponds to Ed::GFP fused to Dsh FL and RNAi against *mud* (**I**); Ed::Dsh + *lis1* RNAi corresponds to Ed::GFP fused to Dsh FL and RNAi against Lis1 (**J**). The scale bar in (**B**) represents 2 μm.

K–L”: Localization of Dsh::Myc (red in **K, K”, L** and **L”**) in S2 cells expressing Ed::GFP (green in **K’, K”**) or Ed::Fz4C (green **L, L’”**). The scale bar in (**K**) represents 2 μm.

M: Cumulative graph of angles measured in the S2 cell “induced polarity” assays in Ed::GFP (black line), Ed::Dsh (blue line); Ed::Dsh(DEP) (green line) and Ed::Dsh(PDZ) (red line).

N: Cumulative graph of angles measured in the S2 cell “induced polarity” assays in Ed::GFP (black line), Ed::Fz1C (dark purple line) and Ed::Fz4C (light purple line).

O: Cumulative graph of angles measured in the S2 “induced polarity” assay in Ed::GFP (black line); Ed::Dsh FL (blue line); Ed::Dsh FL and *dlg* RNAi (orange line); Ed::Dsh FL and *mud* RNAi (green line); Ed::Dsh FL and *lis1* RNAi (purple line).

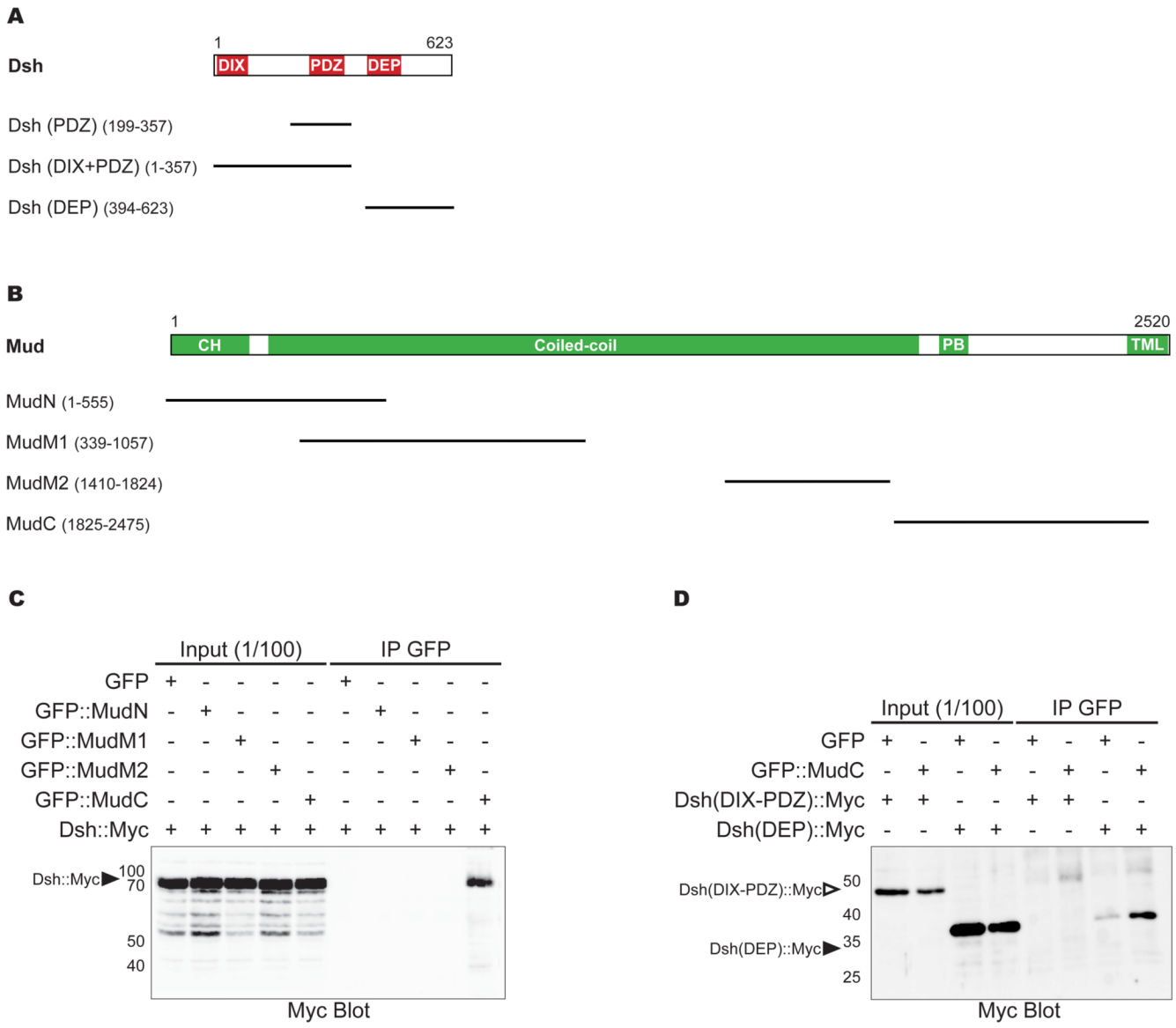

Figure 2. MudC forms a complex with the Dsh DEP domain

A: Schematic of Dsh domains used in the S2 cell "induced polarity" assays and in the immunoprecipitation experiments. The conserved domains are in red: the DIX (Dishevelled/Axin) domain is from amino acids (aa) 8 to 91; the PDZ (PSD-95/DLG/ZO1) domain is from aa 252 to 337; the DEP (Dishevelled/EGL-10/Plextrin) domain is from aa 407 to 476.

B: Schematic of Mud domains used in the immunoprecipitation experiments. The conserved domains are in green: the CH (Calponin homology) domain comprises the first 246 aa; the coiled-coil domains are from aa 246 to 1887; the PB (Pins binding) domain is from aa 1947 to 2001; the putative TML (transmembrane-like) domains are from aa 2410 to 2514. The presence of highly repeated sequence between aa 1058 to 1409 has so far prevented the cloning of this region in expression vectors. The Mud microtubule binding domain is located between aa 1824 and 2001 (Bowman et al., 2006).

C: Anti-Myc antibody Western blot of GFP::MudN, GFP::MudM1, GFP::MudM2 or GFP::MudC immunoprecipates from extracts of HEK293T cells expressing full-length Dsh-Myc. Arrowhead indicates Dsh::Myc.

D: Anti-Myc antibody Western blot of GFP::MudC immunoprecipates in extracts of HEK293T cells expressing Dsh(DIX-PDZ)::Myc or Dsh(DEP)::Myc. Empty and filled arrowheads indicate Dsh(DIX-PDZ)::Myc and Dsh(DEP)::Myc, respectively.

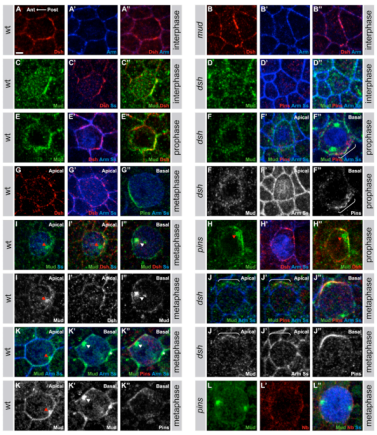

Figure 3. The localization of Mud is dependent on Pins and Dsh

A–B”: Localization of Dsh (red in **A, A”, B, B”**) and Armadillo (blue in **A’, A”, B’, B”**) at the apical cortex of wild-type (**A–A”**) and *mud* mutant (**B–B”**) interphase pI cells; pI cells identified by the accumulation of Senseless (Ss, Nolo et al., 2000). In epithelial cells of the dorsal thorax, Dsh is planar polarized and accumulates weakly at the posterior apical cortex of all epithelial cells and strongly at the apical posterior cortex of the pI cells. Therefore, Dsh appears strongly enriched at the posterior cortex of the pI cell and weakly enriched at the posterior cortex of the epithelial cells located anterior to the pI cells.

C–D”: Apical localization of Mud (green in **C, C”, D, D”**), Dsh (red in **C’, C”**), Armadillo (Arm, blue in **D’, D”**), Senseless (Ss,), blue in **C’, D’, D”**) and Pins (red in **D’, D”**) in wild-type (**C–C”**) and *dsh*^{1} mutant (**D–D”**) in pI cells in interphase. Note that, Mud does not accumulate with Dsh at the posterior apical cortex of the epithelial cells located anterior to the pI cells suggesting that the colocalization between Dsh and Mud is specific to the pI cells, in agreement with the notion that the Fz-Dsh pathway regulates mitotic spindle orientation in the pI cells and not in the epithelial cells (Gho and Schweisguth, 1998).

E–F”: Localization of Mud (green in **E, E”, F–F”**), Dsh (red in **E’, E”**), Armadillo (Arm, blue in **E’, F’, F”**), Senseless (Ss, blue in **E’, F’, F”**) and Pins (red in **F’, F”**) in wild-type (**E–E”**) and *dsh*^{1} mutant (**F–F”**) in pI cells in prophase. Apical confocal sections are shown in **E–F’**. Basal confocal section is shown in **F”**. The bracket in **F”** indicates the accumulation of Pins and Mud at the basal-lateral cortex of the *dsh*^{1} mutant in prophase.

G–G”: Localization of Dsh (red in **G, G’**), Armadillo (Arm, blue in **G’,G”**), Senseless (Ss, blue in **G’,G”**) and Pins (green in **G”**) in wild-type pI cell in metaphase. Apical confocal sections are shown in **G** and **G’** and a basal confocal section is shown in **G”**.

H–H”: Apical localization of Mud (green in **H, H”**), Dsh (red in **H’, H”**), Armadillo (Arm, blue in **H’**), Senseless (Ss, blue in **H’**) in *pins* pI cell in prophase. The red arrowhead indicates the apical centrosome in vicinity of the apical accumulation of both Mud and Dsh.

I–I”: Localization of Mud (green in **I–I”**), Dsh (red in **I’, I”**), Senseless (Ss, blue in **I–I”**) in wild-type pI cell in metaphase. Apical confocal section are shown in **I** and **I’**. Basal confocal section is shown in **I”**. The red arrowhead indicates the apical posterior centrosome in the vicinity of the apical accumulation of Mud. The white arrowhead indicates the basal anterior centrosome in the vicinity of the anterior basal-lateral Mud accumulation.

J–J”: Localization of Mud (green in **J–J”**), Pins (red in **J’, J”**), Senseless (Ss, blue in **J–J”**) and Armadillo (Arm, blue in **J–J”**) in a *dsh*^{1} mutant pI cell in metaphase. Apical confocal sections are shown in **J** and **J’**. Basal confocal section is shown in **J”**. The white brackets in **J** and **J’** indicate the lateral accumulation of Mud, which localizes with Pins (**J’**) along the lateral cortex of the pI cell.

K–K”: Localization of Mud (green in **K–K”**), Pins (red in **K”**), Senseless (Ss, blue in **K–K”**) and Armadillo (Arm, blue in **K–K”**) in a wild-type pI cell in metaphase. An apical

confocal section is shown in **K** and basal confocal sections are shown in **K'** and **K"**. The red arrowhead indicates the apical posterior centrosome in the vicinity of the apical accumulation of Mud. The white arrowhead indicates the basal anterior centrosome in the vicinity of the anterior basal-lateral Mud accumulation. The asterisk (**K'** and **K"**) indicates the centrosome of a dividing neighboring epithelial cell.

L–L": Lateral localization of Mud (green in **L, L"**), Numb (Nb, red in **L', L"**), Senseless (Ss, blue in **L"**) in a *pins* pI cell in metaphase.

In all panels anterior is to the left. Scale bar (**A**) is 2μm.

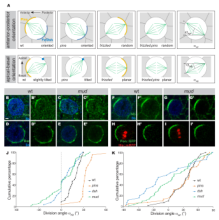

Figure 4. Mud controls mitotic spindle orientation downstream of Fz PCP

A: Schematic of the localization and function of the Fz-Dsh and the Pins for the regulation of the mitotic spindle orientation in the pI cells according to David et al., 2005. pI cells are in white, surrounding epithelial cells are in grey, mitotic spindle is in green. In the pI cell, Fz and Dsh (dark blue) are accumulated at the apical posterior cortex, Pins (orange) is located at the anterior lateral cortex. At the apical posterior pole of the cell, Fz and Dsh control the anterior-posterior orientation of the mitotic spindle. As Fz and Dsh are localized at the apical cortex of the pI cell, they pull the posterior centrosome of the spindle inducing a tilt of the spindle along the apical-basal axis. At the anterior lateral pole of the pI cell, Pins and the HGP pathway, composed of Ric-8, Gαi and Gγ1, act in opposition to Fz and Dsh to maintain the spindle in the plane of the epithelium. In *fz* mutant cells, the spindle is randomly oriented along the anterior-posterior axis and more planar than in wild-type cells. In *pins* mutant cells, there is no defect along the anterior-posterior axis but the spindle is more tilted than in wild-type cells. Since the activity of Pins and the HGP pathway are only needed to counterbalance the Fz PCP pathway, the *fz, pins* double mutant and the *fz* mutant pI cells have a similar phenotype. Schematic of the α_{AP} and α_{AB} angles measured as described in (David et al., 2005).

B–G': Localization of the polarity markers, Pins (green in **B–C'**), Bazooka (Baz, green in **D–E'**), and Numb (Nb, green in **F–G'**) in wild type (**B, B'**, n=26 for Pins localization; **D, D'**, n=32 for Baz localization; **F** and **F'**, n=32 for Numb localization) and *mud* mutant (**C, C'**, n=30 for Pins localization; **E, E'**, n=46 for Baz localization; **G** and **G'**, n=46 for Numb localization) pI cells in metaphase. pI cells are labeled by Senseless (blue, **B, C, D, E, F** and **G**).

H–I': Localization of Pon::GFP (green) in wild type (**H**, n=17) and *mud* mutant (**I**, n=15) pI cells in metaphase. pI cells are labeled by the expression of Histone2B::mRFP (His::mRFP, red in **H** and **I**). Pon::GFP and His::mRFP were expressed under the control of the *neuralized-Gal4* driver.

J: Cumulative plot of α_{AB} (angle of mitotic spindle relative to the plan of the epithelium) in wild type (n=22), *pins* (n=29), *dsh*^{1} (n=24) and *mud* (n=48) mutant pI cells. Measured angles are positive when the anterior pIIb spindle is more basal than the posterior one. We identified the anterior pole during pI cell division as the pole giving rise to pIIb. α_{AB} angles were measured at midpoint between spindle formation and anaphase.

K: Cumulative plot of α_{AP} (angle of mitotic spindle relative to the anterior-posterior axis) in wild type (n=27), *pins* (n=16), *dsh*^{1} (n=24) and *mud* (n=48) mutant pI cells. Measured angles are positive when the anterior spindle pole is closer of the midline than the posterior one. α_{AP} angles were measured at midpoint between spindle formation and anaphase.

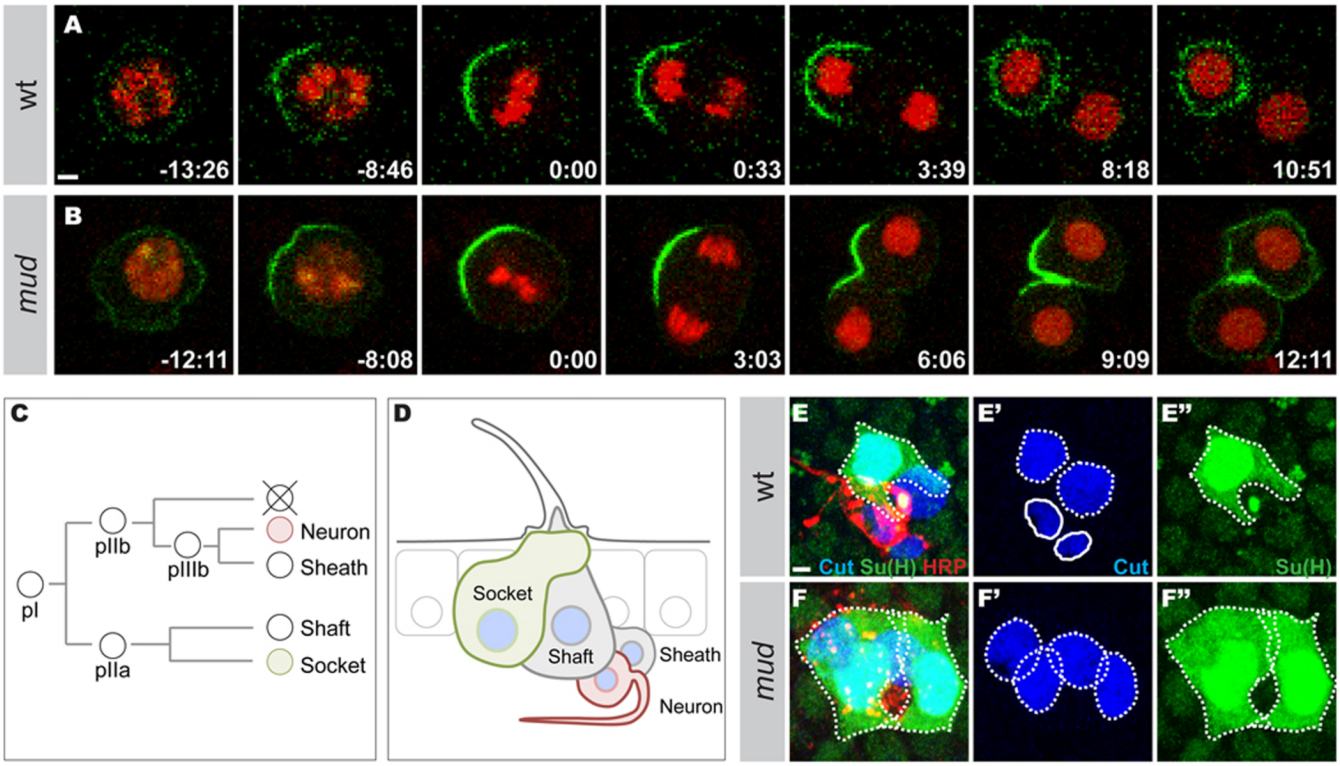

Figure 5. Mud loss of function is associated with Pon::GFP misegregation and cell fate specification defects

A and **B**: Time-lapse of Pon::GFP (green) and Histone2B::mRFP (His::mRFP, red) localizations in a wild type pI cell (**A**) and a *mud* mutant pI cell (**B**). Pon::GFP fails to segregate exclusively in one daughter cell in 26.6% of the *mud* mutant cells (n=15). Pon::GFP and His::mRFP were expressed under the control of the *neuralized-Gal4* driver. Time in minutes:seconds.

C: The pI cell lineage. The pI cell divides asymmetrically to produce a pIIa cell and a pIIb cell. The pIIa generates the external socket and shaft cells. The pIIb gives rise to the neuron and the sheath as well as a cell that undergoes apoptosis. Numb, Pon and Neuralized are inherited by the pIIb cell, the apoptotic cell, the neuron and the shaft cell.

D: Schematic representation of the adult sensory organ. The wild-type sensory organ is composed of 4 cells: the external socket and shaft cells; the internal neuron and sheath cell. Each sensory cell expresses the Cut nuclear marker (blue). The socket cell expresses the Su(H) marker (green) and the neuron expresses the HRP marker (red).

E–F: Sensory organs in wild-type (**E–E”**) and *mud* mutant (**F–F”**) pupae at 24 h APF stained for Cut (blue in **E, E’, F** and **F’**), Su(H) (green in **E, E”, F** and **F”**) and HRP (red in **E** and **F**). All panels are z maximal projections. The wild-type organ (**E**) is composed of four different cells. The external subepithelial socket and shaft cells are identified based on their large subepithelial polyploidy nucleus stained by Cut (dashed outline in **E’**). The socket cells is identified by the expression of the Su(H) marker (dashed outline in **E** and **E”**). The sheath cell and the neuron are identified by their basal position and their smaller nucleus (solid outline in **E’**). The Cut positive sheath cell is located next to the neuron identified by its strong HRP staining (red). A *mud* mutant organ (**F**) is composed of four large Cut positive nucleus (dashed outlines in **F’**), none of which are strongly HRP positive (**F**): two socket cells identified by Su(H) staining (green, dashed outlines in **F** and **F”**) and two subepithelial Cut positive cells identified as a shaft cell based on their large

subepithelial polyploid nuclei. The percentage of cell fate transformation is 1.6% in *mud* mutant pupae (n = 180 organs).
Scale bars are 2μm and anterior is left.

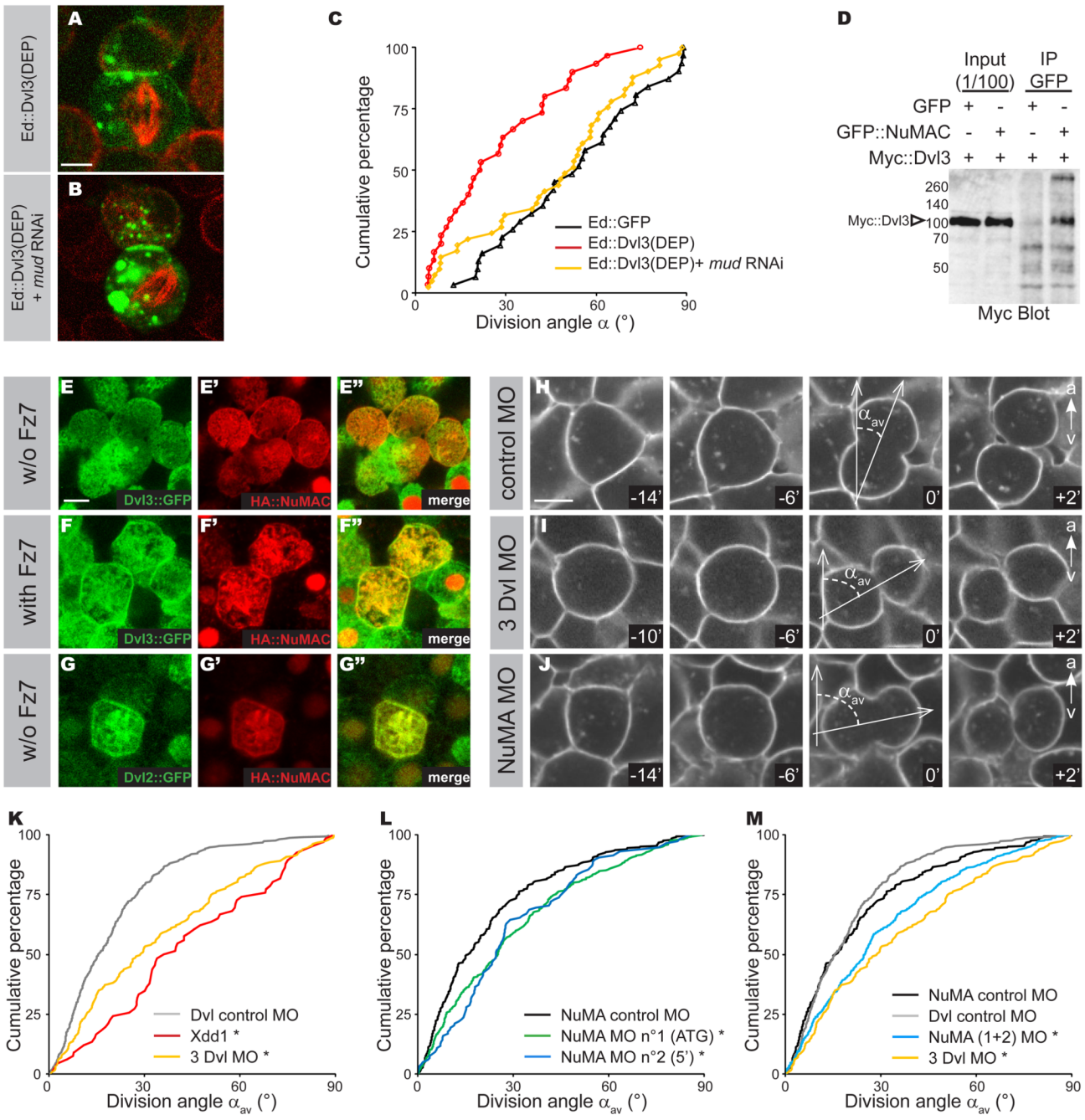

Figure 6. NuMA controls mitotic spindle orientation downstream of the Fz PCP pathway during zebrafish gastrulation

A and **B**: Dvl3(DEP), C-terminal region of Dvl3 containing the DEP domain was fused in frame to Echinoid tagged with GFP (green) and transfected into S2 cells. Cells were stained for α-tubulin (red). Ed::Dvl3(DEP) (**A**) ; Ed::Dvl3(DEP) + *mud* RNAi corresponds to Ed::GFP fused to Dvl3(DEP) and RNAi against *mud* (**B**). The scale bar in (**A**) represents 2 μm.

C: Cumulative plot of angles measured in the S2 cell "induced polarity" assays in Ed::GFP (black line), Ed::Dvl3(DEP) (red line); Ed::Dsh(DEP) and *mud* RNAi (yellow line).

D: Anti-Myc antibody Western blot of GFP::NuMAC immunoprecipates from extracts of HEK293T cells expressing full-length Dvl3::Myc. Arrowhead indicates Dvl3::Myc.
E–G: Localization of Dvl and NuMAC in epiblast cells during gastrulation. Localization of Dvl3::GFP (green in **E** and **E”**) and HA::NuMAC (red in **E’** and **E”**) in interphasic and dividing epiblast cells without Fz7 co-injection. Localization of Dvl3::GFP (green in **F** and **F”**) and HA::NuMAC (red in **F’** and **F”**) in interphasic and dividing epiblast cells with Fz7 co-injection. Cortical enrichment of HA::NuMAC was observed in 7 of 14 epiblast cells in division in absence of Fz7, whereas most of the dividing epiblast cells (12 out of 14) have a strong cortical localization and cytoplasmic depletion of HA::NuMAC when Dvl3::GFP was strongly enriched at the cortex upon Fz7 co-injection. Localization of Dvl2::GFP (green in **G** and **G”**) and HA::NuMAC (red in **G’** and **G”**) in a dividing epiblast cells in absence of Fz7 co-injection. Scale bar is 10 μm (**E**).
H–J: Confocal time-lapse images of embryos labeled with membrane-GFP and injected with the control morpholino (**H**) or the triple Dvl MO (**I**) or the NuMA ATG morpholino (**J**). Observations are done on the dorsal side, from shield stage to 80% epiboly, and limited to the neuro-ectoderm. Scale bars is 10 μm (**H**) and animal pole is to the top. Time is in minutes.
K–M: Cumulative plot of α_{av} in embryos injected with the Dvl control morpholino (n=304 divisions in 5 embryos), or the Xdd1 construct (n=66, in 1 embryo, already shown by Gong et al., 2004) or the three Dvl morpholinos (n=183, in 4 embryos) (**K**); Cumulative plot of α_{av} in embryos injected with the NuMA control morpholino (n=304 divisions in 5 embryos), the NuMA “ATG” morpholino (n=339 divisions in 9 embryos), the NuMA “5’ ” morpholino (n=118 divisions in 3 embryos) (**L**); Cumulative plot of α_{av} in embryos injected with the NuMA control morpholino (n=304 divisions in 5 embryos), the Dvl control morpholino (n=183 divisions in 4 embryos), the NuMA “ATG” morpholino (n=339 divisions in 9 embryos) and the NuMA “5’ ” morpholino (n=118 divisions in 3 embryos) pooled together or triple Dvl morpholino (n=183, in 4 embryos) (**M**); Asterisk indicates $p<0.001$ relative to control experiments.

Table 1

Echinoid fusion protein spindle orientation ability

Echinoid::GFP fusion partner	Average Angle	Standard Deviation	n
None	52.8	23.3	31
Dsh	27.8	17.9	45
Dsh + *dlg* RNAi	20.8	17.4	25
Dsh + *mud* RNAi	46.0	26.6	38
Dsh + *lis-1* RNAi	43.3	25.3	32
Dsh (DEP)	16.9	14.9	69
Dsh (PDZ)	48.5	24.0	18
Fz1 (C-ter)	46.2	28.9	33
Fz4 (C-ter)	24.1	12.1	22
Dvl3 (DEP)	27.4	19.9	30
Dvl3 (DEP) + *mud* RNAi	46.3	24.9	41